Journal of Applied Physics

Damping of Underwater Explosion Bubble Oscillations

Cite as: Journal of Applied Physics **27**, 1152 (1956); https://doi.org/10.1063/1.1722221
Submitted: 26 March 1956 • Published Online: 14 May 2004

Joseph B. Keller and Ignace I. Kolodner

View Online Export Citation

ARTICLES YOU MAY BE INTERESTED IN

Bubble oscillations of large amplitude
The Journal of the Acoustical Society of America **68**, 628 (1980); https://doi.org/10.1121/1.384720

An integrated wave-effects model for an underwater explosion bubble
The Journal of the Acoustical Society of America **111**, 1584 (2002); https://doi.org/10.1121/1.1458590

Nonlinear bubble dynamics
The Journal of the Acoustical Society of America **83**, 502 (1988); https://doi.org/10.1121/1.396145

AIP Publishing

© 1956 American Institute of Physics.

position a V-shaped glass tube of 8-mm inside diameter was connected to the capillary end by means of a ground joint. This was ground directly on the capillary end, and this device, shown in Fig. 2, served the same purpose as placing the ends under water. Comparison with directly immersed tubes showed that there was no detectable error in this method.

Three runs were made under the same conditions each time, and the average values were taken into account. The agreement and the reproducibility of the different runs were very good, and there was one capillary tube for comparison in all experiments both with untreated and treated capillaries—no error due to timing, etc., remained.

The mean diameter of the tubes was measured by weighing the amount of mercury necessary to fill them. The capillary tubes were of Pyrex, and as they varied slightly in diameter the values given are averages.

First the experiments were done under various pressures, using the capillary tubes cleaned with chromic acid cleaning solution. One capillary was then removed, dried on the respirator pump, and treated with dimethyldichlorosilane vapor. With that capillary and the untreated one, which had not been changed, a second run was made in the same way and the results were compared with the previous ones.

The results for a series of different capillaries are shown in the Diagrams in Figs. 3 to 6. In order to make comparison of the results easier, two curves have been drawn in one diagram but the abscissa for the second curve has been shifted horizontally very slightly. The break in the curves shown in Figs. 4 and 5 shows the beginning of turbulent flow. The mean velocity where this turbulent flow starts agrees in magnitude with that calculated from Reynold's[15] equation

$$\bar{v}=R\frac{\eta}{2r\rho},$$

where R was set at 2300 and

η = the viscosity of water for 30°

r = the radius of the tube and

ρ = the density of water at 30°.

In an experiment, the results of which are shown in Fig. 6, the conditions for turbulent flow were not reached because of the small diameter of the tubes, but at higher pressure (400 mm Hg, not shown in the diagram) the values for the treated and untreated capillary tube coincide. This shows that in the above case the friction on the glass surface is already so high that no distinction is possible.

ACKNOWLEDGMENTS

The author wishes to express his thanks to Professor E. G. Rochow who suggested this problem and made many valuable suggestions for its solution.

JOURNAL OF APPLIED PHYSICS VOLUME 27, NUMBER 10 OCTOBER, 1956

Damping of Underwater Explosion Bubble Oscillations*

JOSEPH B. KELLER AND IGNACE I. KOLODNER†
Institute of Mathematical Sciences, New York University, New York, New York

(Received March 26, 1956)

When an explosive detonates underwater it creates a bubble of gas which performs damped radial oscillations of large amplitude. The usual theory of these oscillations treats the water as incompressible and yields undamped oscillations of constant period. We have modified this theory by taking account of the compressibility of the water. Our theory predicts damped oscillations of diminishing period. Comparison of the predicted and observed radius-time curves for one particular case shows fairly good agreement. Radius-time curves for four representative cases have been computed with a large number of periods in each case. These can be used to describe a variety of explosions.

1. INTRODUCTION

DETONATION converts an explosive into a gas at high pressure. When the explosion occurs underwater this gas is called the "bubble." It expands rapidly until its pressure falls to that of the surrounding water but inertia causes it to overexpand. After it ceases expanding, the pressure of the surrounding water compresses it until it again attains a high pressure. Then the cycle of expansion and contraction begins once more, and repeats continually with oscillations of diminishing amplitude. As the bubble oscillates and its pressure varies, pressure waves are transmitted outward into the water. These pressure waves, the first of which is a shock, cause the damage done by the explosion and account for the damping of the bubble oscillations.

* This article represents results obtained at the Institute of Mathematical Sciences, New York University, under the auspices of Contract Nonr-285(02) with the Office of Naval Research. Some of the results were originally presented at the Fourth Conference on Progress in Research on Ship Protection against Underwater Explosions in December, 1951.

† Present address: Department of Mathematics, The University of New Mexico, Albuquerque, New Mexico.

The usual theory of these bubble oscillations[1] is based on the assumption that the water is incompressible and it consequently predicts undamped oscillations of constant period. We have modified the theory by taking the compressibility of the water into account, and we then find damped oscillations of diminishing period. On the basis of this modified theory we have calculated a number of curves of bubble radius *versus* time. One of these is shown in Fig. 7, along with the corresponding experimental points. The agreement between theory and experiment can be seen to be fairly good. The radius-time curves and pressure data shown in Figs. 3 through 6 and Tables I–IV correspond to various explosions, i.e., various charge weights and depths. They were computed on the UNIVAC, an electronic digital computer, at New York University and a program is available on tape for computing similar curves for other explosions. However, by using the curves presented here and the qualitative results of Sec. 4, it is possible to obtain radius-time curves for a wide range of explosions without additional calculation.

The theory which we have used is very similar to that of K. Zoller.[2] He used the theory to calculate the pressure waves produced by the explosion and found them to be in excellent agreement with the waves obtained by numerical integration of the equations of motion of water. He also calculated two cycles of the radius-time curve for one particular explosion.

The novel feature of the theory is the use of the wave equation, rather than the customary Laplace equation, for the potential function ϕ of the water. The wave equation is closer than is the Laplace equation to the exact equation for ϕ, which is

$$\nabla^2\phi - c^{-2}\phi_{tt} = \frac{1}{2c^2}\left[\frac{d}{dt}(\nabla\phi)^2 + \frac{\partial}{\partial t}(\nabla\phi)^2\right].$$

This can be seen by noting that if the terms on the right in the above equation are dropped, which is permissible if the particle velocities are small compared to the sound speed c, then the wave equation results. Laplace's equation remains if the term $c^{-2}\phi_{tt}$ is also dropped. A test of the agreement between a flow based on the wave equation and an exact flow was made by G. I. Taylor.[3] He considered the flow produced by a uniformly expanding sphere, and found excellent agreement even for very large (i.e., nearly sonic) velocities of the sphere.

An early theory of the damping of the bubble oscillations was given by C. Herring.[4] He assumed that the usual incompressible theory adequately described the oscillations. Then he estimated the rate of energy loss from the bubble by assuming that the pressure waves were acoustic. Our theory likewise treats the pressure waves as acoustic, but takes account of their effect on the bubble motion. In this connection nonlinearity is introduced into the theory.

We wish to thank Mrs. Halina Montvilla and Mrs. Susan Hahn for performing the hand calculations on which Figs. 7–9 are based and Dr. Phyllis Fox and Mr. Louis Brathwaite for programming Eq. (12) for the UNIVAC and calculating the results shown in Figs. 3–6 and Tables I–IV.

2. FORMULATION

We consider a sphere of gas (the bubble) of initial radius a_0 surrounded by an unbounded fluid (the water) initially at rest. We assume that the bubble remains spherical at all later times, that the pressure throughout the bubble is constant at each instant of time t and that the pressure P in the bubble is related to its radius $a(t)$ by the adiabatic relation

$$P(a) = k\left[\frac{4\pi}{3}a^3\right]^{-\gamma}. \tag{1}$$

We further assume that the water velocity is derivable from a potential function $\phi(r,t)$ which depends only upon radial distance r from the bubble center and upon time t, and satisfies the wave equation

$$\nabla^2\phi - \frac{1}{c^2}\phi_{tt} = 0. \tag{2}$$

Here c is the sound speed in the fluid, assumed to be constant. The pressure $p(r,t)$ in the water is given by the Bernoulli equation

$$p(r,t) = p_0 - \rho(\phi_t + \tfrac{1}{2}\phi_r^2). \tag{3}$$

Here ρ is the density of the fluid and p_0 is its initial pressure.

At the bubble surface, pressure must be continuous and the rate of change of bubble radius must equal the particle velocity in the water. Before writing these conditions we introduce the reduced pressure difference $\Delta(a)$ by the definition

$$\Delta(a) = \rho^{-1}[P(a) - p_0]. \tag{4}$$

Then the boundary conditions become

$$\Delta(a) = -(\phi_t + \tfrac{1}{2}\phi_r^2) \quad \text{at} \quad r = a(t) \tag{5}$$

$$\dot{a} = \phi_r \quad \text{at} \quad r = a(t). \tag{6}$$

The problem is to solve (2), (5), and (6) for $\phi(r,t)$ and $a(t)$ given that the initial bubble radius and velocity

[1] R. H. Cole, *Underwater Explosions* (Princeton University Press, Princeton, 1948).

[2] K. Zoller, "Adiabatically pulsating gas bubbles in an infinitely extended compressible fluid," Stuttgart-Ruit, July, 1942. Halstead Exploiting Center 11666.

[3] G. I. Taylor, Proc. Roy. Soc. (London) (A), **186**, 273–292 (1946).

[4] C. Herring, "Theory of the pulsations of the gas globe produced by an underwater explosion," NDRC Div. 6, Report C4-sr20 (1941).

are a_0 and $\dot{a}_0$ and that the fluid is initially at rest, i.e.,

$$a(0)=a_0, \quad \dot{a}(0)=\dot{a}_0, \quad \phi(r,0)=0, \quad r>a_0; \qquad \phi_t(r,0)=0, \quad r>a_0. \tag{7}$$

It is to be noted that the initial bubble velocity $\dot{a}_0$ may differ from zero, even though the fluid away from the bubble is at rest. This is possible in a compressible fluid but not in an incompressible one. In the incompressible theory c is infinite so that $(1/c^2)\phi_{tt}$ in (2) does not appear, and therefore the initial conditions on ϕ and ϕ_t are replaced by the vanishing of ϕ at $r=\infty$. The problem is otherwise the same, and its solution can be obtained by specializing our result.

3. SOLUTION

To solve (2), (5), (6), and (7) we choose a particular solution of (2), namely

$$\phi=\frac{f(\zeta(t,r))}{r}, \quad \zeta=t-\frac{r-a_0}{c}. \tag{8}$$

Then (5) and (6) become

$$\Delta(a)=-a^{-1}f'(\zeta(t,a))-\tfrac{1}{2}\dot{a}^2 \tag{9}$$

$$\dot{a}=-a^{-2}f(\zeta(t,a))-(ac)^{-1}f'(\zeta(t,a)). \tag{10}$$

Eliminating $f'(\zeta(t,a))$ between (9) and (10) and differentiating the result with respect to t yields

$$(\dot{a}-c)f'(\zeta(t,a))+[(\tfrac{1}{2}\dot{a}^2+\Delta(a)-c\dot{a})a^2]^{\cdot}=0. \tag{11}$$

Now eliminating $f'(\zeta(t,a))$ between (9) and (11) and simplifying yields

$$(\dot{a}-c)(+a\ddot{a}+\tfrac{3}{2}\dot{a}^2-\Delta)-\dot{a}^3+a^{-1}(a^2\Delta)^{\cdot}=0. \tag{12}$$

Equation (12) is a nonlinear second-order ordinary differential equation for $a(t)$, and the initial data are given in (7). Once $a(t)$ is known, f and f' can be determined from (9) and (10), which yield

$$f(\zeta(t,a))=-a^2\dot{a}+\frac{a^2}{c}\left(\frac{\dot{a}^2}{2}+\Delta\right), \tag{13}$$

$$f'(\zeta(t,a))=-a\left(\frac{\dot{a}^2}{2}+\Delta\right). \tag{14}$$

Then p can be found from (3) and (8) which yield

$$[p(r,t)-p_0]/\rho=-\frac{f'}{r}-\frac{f^2}{2r^4}-\frac{1}{2c}\left(\frac{f'^2}{cr^2}+\frac{2ff'}{r^3}\right). \tag{15}$$

If we neglect terms of order c^{-1} in (15) it becomes

$$p(r,t)=p_0-\rho\left[\frac{f'}{r}+\frac{f^2}{2r^4}\right]. \tag{16}$$

Now using (13) to compute f and f' to order c^{-1}, we obtain

$$p(r,t)=p_0-\rho\left[-\frac{(a^2\dot{a})^{\cdot}}{r}+\frac{(a^2\dot{a})^2}{2r^4}\right]. \tag{17}$$

Eq. (17) is of exactly the same form as that given by the incompressible theory, in which $c=\infty$, but the function $a(t)$ is different in that theory. Furthermore, in (13), which was used in obtaining (17), the argument of f is $\zeta(t,a(t))$ rather than $\zeta(t,r)$. But $\zeta(t,r)=\zeta(x,a(x))$ if x is defined by

$$x=t-\frac{r}{c}-\frac{a(x)}{c}\approx t-\frac{r}{c}. \tag{18}$$

Thus in (17) a must be evaluated at $t-r/c$. This shows that the pressure waves travel outward with the finite speed c. If (13) and (14) are used to compute p from (16), the retarded time $t-r/c$ must also be used in (13) and (14).

The term $-(a^2\dot{a})^{\cdot}r^{-1}$ in (17) is important near bubble minima, and it accounts for the pressure in the primary shock wave and the subsequent pressure peaks. The term $(a^2\dot{a})^2/2r^4$ is called the "afterflow" pressure. It is important between pressure peaks, but only at small distances from the bubble. Finally, we note that Eq. (17) takes on the following simple form in terms of the bubble volume V

$$p(r,t)=p_0+\rho\left[\frac{\ddot{V}\left(t-\frac{r}{c}\right)}{4\pi r}-\frac{\dot{V}^2\left(t-\frac{r}{c}\right)}{32\pi^2r^4}\right]. \tag{19}$$

4. THE RADIUS-TIME CURVE

We have already seen that the pressure and velocity of the water can be expressed in terms of the bubble radius $a(t)$, which is a solution of (12). Therefore we must solve this second-order equation in order to complete the solution of the problem. Since t does not occur explicitly in (12), we can reduce it to a first order equation for $\dot{a}$, which we denote by $v(a)$,

$$\dot{a}=v(a). \tag{20}$$

Then (12) becomes

$$v'(a)=\frac{h(v,a)}{av(c-v)}, \tag{21}$$

where

$$h(v,a)=\tfrac{1}{2}(v^3-3cv^2+2v[\Delta+a\Delta']+2c\Delta). \tag{22}$$

In terms of $v(a)$, the solution for the bubble radius as a function of time is given implicitly by

$$t=\int_{a_0}^{a}\frac{da}{v(a)}. \tag{23}$$

We have found it more convenient, in calculating $a(t)$, to use (12) directly rather than (21) and (23).

However (21) is more useful for the determination of the qualitative behavior of the solution, which we will now consider. The direction field in the (a,v) plane, determined by the right side of (21), has a vortex singularity at the point

$$v=0, \quad a=\bar{a}\equiv\left(\frac{3}{4\pi}\right)^{\frac{1}{3}}\left(\frac{k}{p_0}\right)^{\frac{1}{3\gamma}}. \tag{24}$$

Here $\bar{a}$ is the radius at which $\Delta=0$, i.e. at which the bubble pressure is the same as that in the surrounding fluid. We will call $\bar{a}$ the equilibrium radius. Furthermore v' becomes infinite on the three lines $a=0$, $v=0$ and $v=c$ and it is zero on the line $h(v,a)=0$. Its sign changes on crossing each of these lines.

The equation $h(v,a)=0$ can be solved explicitly for a in terms of v, after $\Delta(a)$ is eliminated from $h(v,a)$ by means of (4) and (1). The result is

$$\sigma a^{3\gamma}=2(3\gamma-1)\left(v-\frac{c}{3\gamma-1}\right)\Big/ \left[v^3-3cv^2-2\alpha c^2(v+c)\right]. \tag{25}$$

In (25) we have introduced the constants σ and α which are defined by

$$\sigma=\frac{\rho}{k}\left(\frac{4\pi}{3}\right)^{\gamma}, \quad \alpha=\frac{p_0}{\rho c^2}. \tag{26}$$

Since a must be positive, we need consider only that portion of the curve (25) for which the right side is positive. The denominator of the right side of (25) is positive for large positive values of v and negative for large negative values of v. It has only one root, which we will vall $\bar{v}$, if $\alpha\leq\frac{3}{2}(3+2\sqrt{3})\approx 9.69$, and this root lies in the interval $3c<\bar{v}<3c[1+(8/27)\alpha]$. It then follows that the curve (25) is defined only in the regions $v<c/(3\gamma-1)$ and $v>\bar{v}$, and that $a\to\infty$ only as $v\to\bar{v}$. Furthermore the derivative with respect to v of the right side of (25) has only one zero in the regions where the curve is defined provided that $\gamma>1$. Therefore the graph of $h(v,a)=0$ is as shown in Fig. 1. We see that this curve has a horizontal slope at the point $v=c/(3\gamma-1)$, $a=0$ where the direction field has a saddle point. In case $\alpha>9.69$ the curve $h(v,a)=0$ is slightly different from that shown in Fig. 1, but the following conclusions concerning the integral curves are the same.

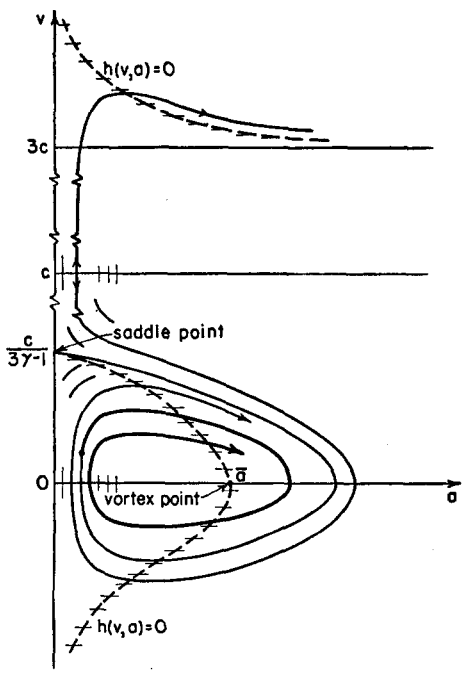

FIG. 1. The direction field in the phase plane for bubble radius oscillations, based upon Eq. (21). The abscissa is the bubble radius a and the ordinate is the velocity $v=\dot{a}$. The curves spiral around the vortex point at $v=0$, $a=\bar{a}$, and tend toward it. This point represents the equilibrium of the bubble.

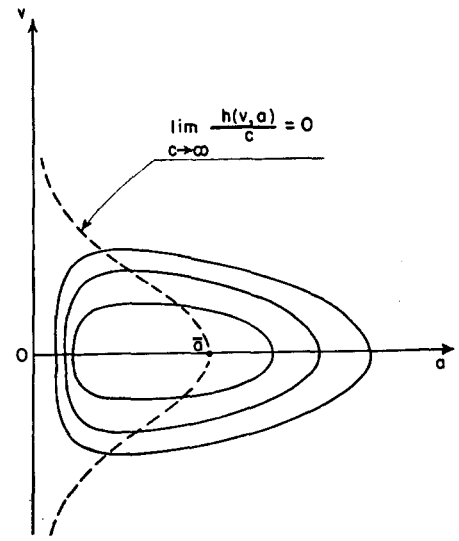

FIG. 2. The direction field in the phase plane for bubble radius oscillations in an *incompressible* fluid. This figure is based upon Eq. (21), with $c=\infty$. The curves are closed and enclose the equilibrium point $v=0$, $a=\bar{a}$.

There are two integral curves passing through the saddle point. One of these is the line $a\equiv 0$ and the other is a spiral which starts with a horizontal slope at the saddle point and spirals clockwise around the vortex point, tending toward it. Consequently all other integral curves also spiral clockwise around the vortex point and tend toward it, as is shown in Fig. 1. In the (a,t) plane these spirals correspond to damped oscillations of the radius which tends toward the equilibrium radius $\bar{a}$. This is exactly the behavior observed in practice. On the other hand, when c is infinite, (21) becomes the equation of the incompressible theory and has only a vortex singularity at $v=0$, $a=\bar{a}$. The direction field for this case is, as shown in Fig. 2, symmetric with respect to the a axis, and all integral curves are closed. All solutions are then periodic undamped oscillations.

It may be verified that for $|v|<c$ the direction field is flatter in the region of negative v than in the region of positive v. A consequence of this is that the bubble's radial velocity always remains smaller than the maximum which it attains in the first expansion. In particular, if the bubble motion starts from rest, this maximum is substantially less than $c/3\gamma-1\sim 0.36c$.

The preceding conclusions about the bubble radius as a function of time can be verified explicitly if the initial bubble radius is near the equilibrium radius $\bar{a}$. In this case the oscillations will be of small amplitude, and can be analyzed by linearization of (12). To this end we write

$$a(t)=\bar{a}+b(t). \tag{27}$$

Upon inserting (27) into (12) and retaining only linear terms in b on the assumption that b is small, we obtain

$$\ddot{b}+\frac{3\gamma p_0}{\rho c\bar{a}}\dot{b}+\frac{3\gamma p_0}{\rho\bar{a}^2}b=0. \tag{28}$$

The general solution of (28) is, with B and θ constants,

$$b(t)=B\exp\left(-\frac{3\gamma p_0}{2\rho c\bar{a}}t\right)\times\cos\left\{\left[\frac{3\gamma p_0}{\rho\bar{a}^2}\left(1-\frac{3\gamma p_0}{4\rho c^2}\right)\right]^{\frac{1}{2}}t+\theta\right\}. \tag{29}$$

The solution (29) describes an exponentially damped sinusoidal oscillation. During one period the amplitude decreases by the factor $\exp(-\pi\sqrt{3\gamma\alpha})$ provided that $\alpha=p_0/\rho c^2\ll 4/3\gamma$.

5. NUMERICAL CALCULATION

In order to determine a radius-time curve the constants a_0, $\dot{a}_0$, p_0, k, γ, ρ, and c must be known. For water at 20°C and atmospheric pressure $\rho=1$ g/cm^3 and $c=1485$ meters/sec. The constant γ depends upon the nature of the explosive, and its value lies between 1 and 1.4. We have used $\gamma=1.25$ in our calculations. The constant k depends upon the nature and amount of explosive, while p_0 is just the hydrostatic pressure at the depth of the explosion. The initial bubble radius and velocity depend upon the size of the explosive and the phase of the oscillation at which the calculation begins. If the calculation begins at a minimum or maximum, then $\dot{a}=0$. However if the calculation begins at the instant of detonation, then $\dot{a}_0$ may have a positive value because a shock wave immediately forms in the water at the bubble surface. One way of finding $\dot{a}_0$ is by considering the conditions at the shock and at the gas-water interface. This method is not necessarily the best since wave motion in the gas within the bubble is neglected in our theory. In any case, the initial bubble radius is very nearly a minimum and should probably be treated as such, as in the incompressible theory.

It is convenient to introduce $\bar{a}$ as the unit of length and $T=\bar{a}(\rho p_0^{-1})^{\frac{1}{2}}$ as the unit of time in order to simplify the computational procedure. The sound speed c' is

TABLE I. Computed values of a_m = minimum radius, a_M = maximum radius, and of $-f'=r\rho^{-1}\cdot$ peak excess pressure $=r\rho^{-1}(p-p_0)$, for an explosion at a depth of 50 feet below the water surface. Units are the same as in Figs. 3–6; $c=94.26$.

t	a_M or a_m	$-f'$
0	5	
4.62	0.08	1149
6.74	2.21	
8.90	0.25	45.3
10.95	1.97	
12.81	0.33	21.5
14.78	1.83	
16.55	0.39	13.3
18.45	1.73	
20.18	0.44	9.32
22.03	1.65	
23.74	0.48	7.03
25.55	1.59	
27.23	0.52	5.55
29.01	1.54	
30.68	0.55	4.52
32.43	1.49	
34.10	0.58	3.77
35.82	1.45	
37.50	0.61	3.21
39.19	1.41	
40.88	0.64	2.77
42.55	1.38	
44.23	0.66	2.41
45.88	1.35	
47.57	0.68	2.13
49.21	1.32	
50.89	0.70	1.89
52.51	1.30	
54.20	0.72	1.68
55.81	1.28	
57.50	0.74	1.51
59.09	1.26	
60.79	0.76	1.36
62.37	1.25	
64.08	0.78	1.24

TABLE II. Same as Table I, for a depth of 100 feet; $c=74.47$.

t	a_M or a_m	$-f'$
0	5	
4.63	0.08	978
6.65	2.12	
8.78	0.28	32.0
10.70	1.89	
12.56	0.37	15.4
14.39	1.74	
16.22	0.43	9.52
17.99	1.65	
19.76	0.49	6.67
21.48	1.57	
23.25	0.54	5.01
24.92	1.51	
26.67	0.58	3.95
28.33	1.46	
30.06	0.62	3.21
31.71	1.41	
33.42	0.65	2.66
35.06	1.37	
36.76	0.68	2.25
38.39	1.34	
40.09	0.70	1.93

TABLE III. Same as Table I, for a depth of 300 feet; $c=47.00$.

t	a_M or a_m	$-f'$
0	5	
4.65	0.10	568
6.50	1.94	
8.55	0.36	16.2
10.32	1.72	
12.16	0.46	7.92
13.87	1.58	
15.66	0.54	4.92
17.34	1.49	
19.09	0.61	3.32
20.75	1.40	
22.46	0.67	2.50
24.10	1.34	
25.79	0.72	1.94
27.43	1.28	
29.08	0.77	1.25
30.71	1.23	
32.35	0.80	1.02
33.98	1.19	
35.60	0.83	0.81
37.23	1.16	
38.84	0.85	0.70
40.46	1.14	
42.08	0.87	0.44

TABLE IV. Same as Table I, for a depth of 1000 feet; $c=26.72$.

t	a_M or a_m	$-f'$
0	5	
4.70	0.13	291
6.46	1.74	
8.36	0.48	7.06
10.06	1.52	
11.79	0.60	3.42
13.43	1.38	
15.14	0.69	2.09
16.75	1.30	
18.45	0.76	1.41
20.05	1.23	
21.73	0.81	1.00
23.32	1.18	
24.99	0.85	0.74
26.58	1.14	
28.24	0.88	0.55

then replaced by the dimensionless sound speed $c=c'(\rho p_0^{-1})^{\frac{1}{2}}$. If a and t are expressed in terms of these units, (12) becomes

$$(\dot{a}-c)(a\ddot{a}+\tfrac{3}{2}\dot{a}^2-a^{-3\gamma}+1)-\dot{a}^3 - (3\gamma-2)a^{-3\gamma}\dot{a}-2\dot{a}=0. \quad (30)$$

The advantage of using these units is that now only c, a_0, $\dot{a}_0$, and γ need be specified to compute a radius-time curve. The other parameters (p_0,ρ, and k) have been absorbed into the units.

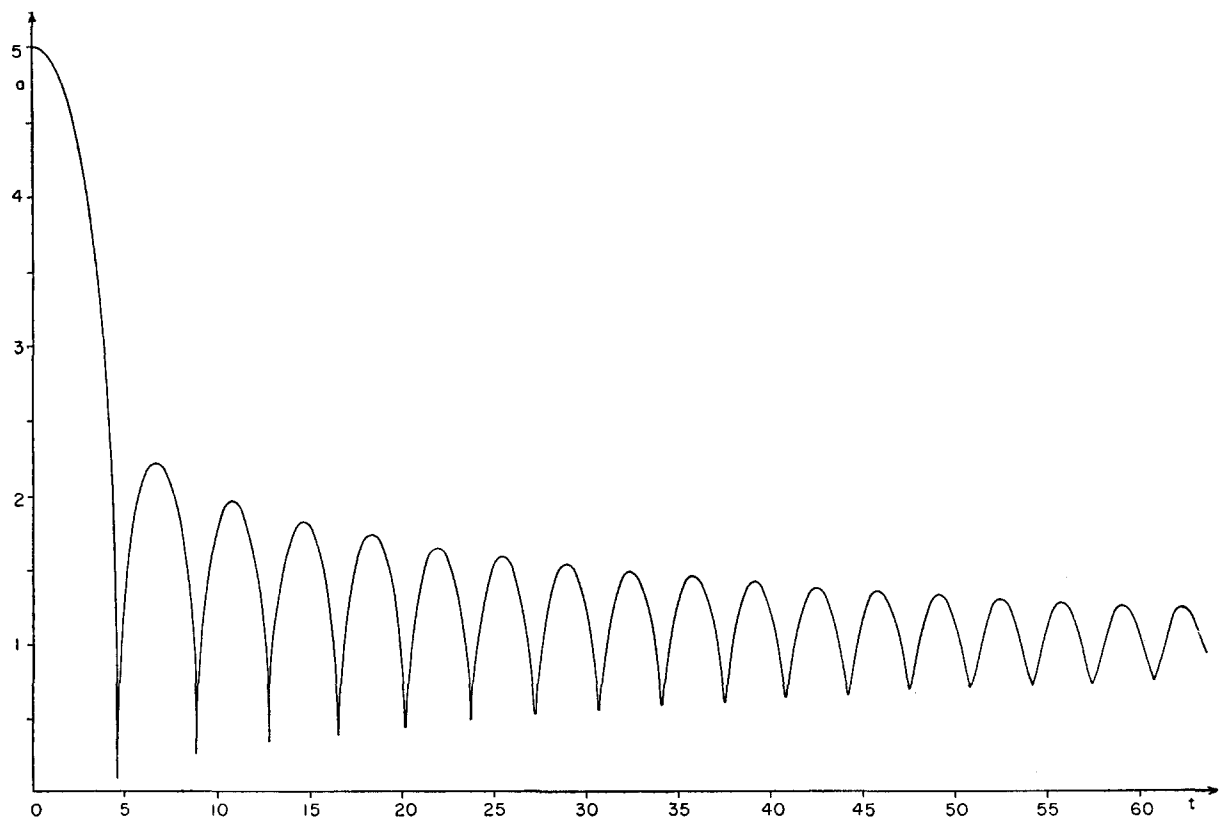

FIG. 3. The bubble radius as a function of time for an explosion at a depth of 50 feet below the water surface. The unit of length is $\bar{a}$, the equilibrium radius of the bubble, which is given in Eq. (24). The unit of time is $\bar{a}(\rho p_0^{-1})^{\frac{1}{2}}$ where ρ is the density of water and p_0 is the hydrostatic pressure at the explosion depth. This curve was computed from Eq. (28) with the initial radius $a_0=5$ (in units of $\bar{a}$) and the initial velocity zero. The values of a at the maxima and minima and the times at which they occur are shown in Table I.

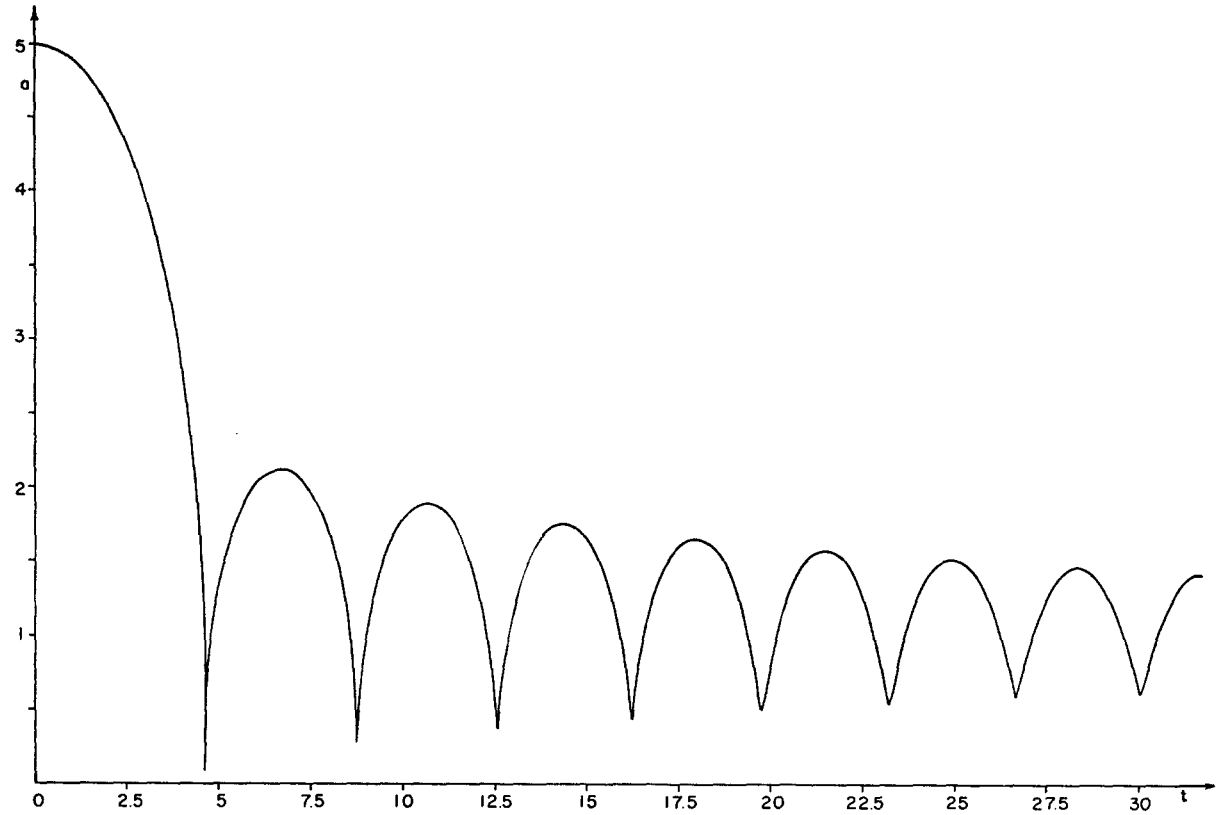

FIG. 4. Same as Fig. 3, for a depth of 100 feet. For data at peaks see Table II.

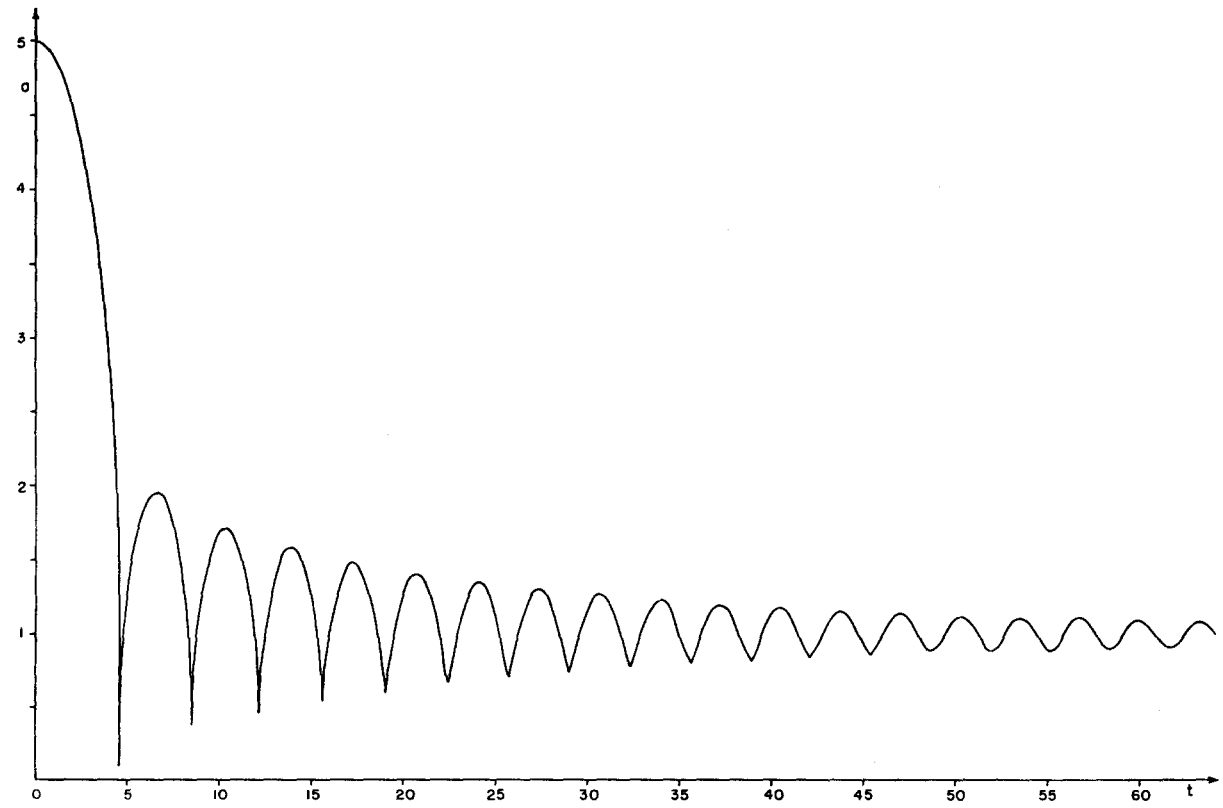

FIG. 5. Same as Fig. 3, for a depth of 300 feet. For data at peaks see Table III.

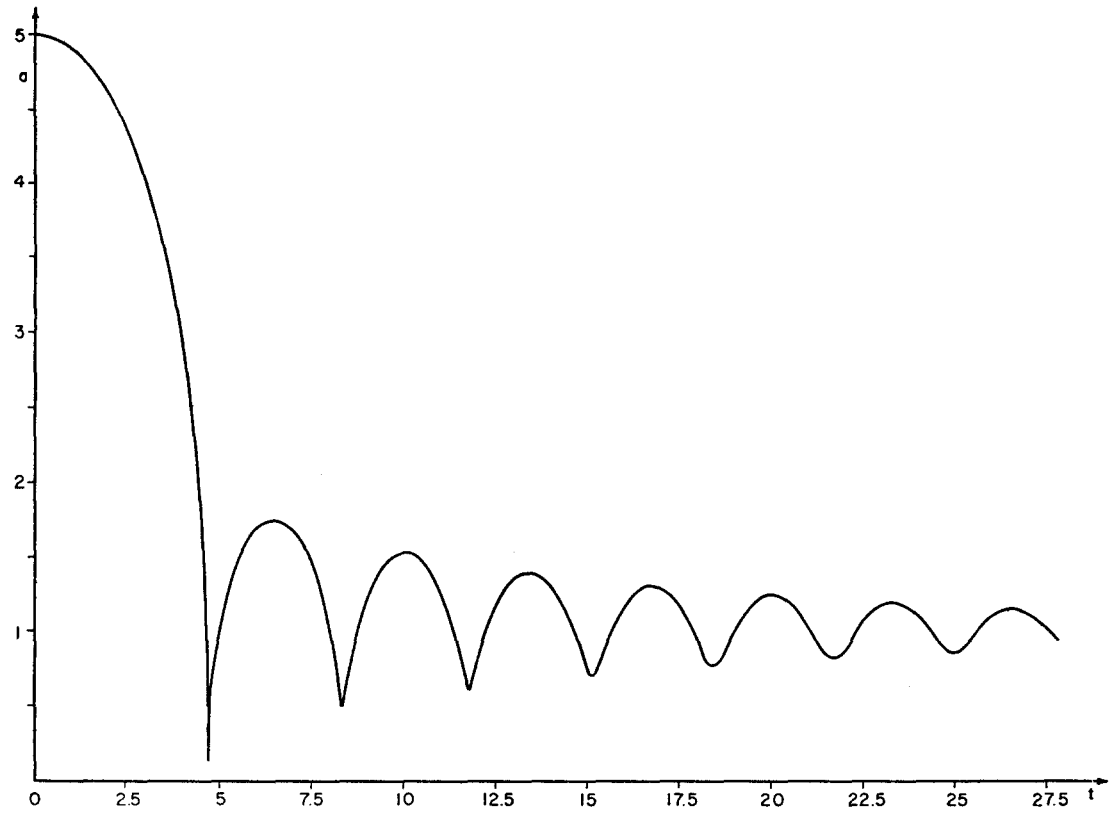

FIG. 6. Same as Fig. 3, for a depth of 1000 feet. For data at peaks see Table IV.

We have chosen $\gamma=1.25$ and considered four representative depths—50, 100, 300, and 1000 feet. For each depth we have computed one radius-time curve using the initial data $a_0=5$, $\dot{a}_0=0$. The number of cycles computed in each case is rather large, as is shown in Tables I–IV. Graphs of the radius as a function of time are shown in Figures 3–6. The successive maximum and minimum values of the radius and the corresponding peak pressure values are given in the tables.

Suppose we wish to determine the radius-time curve

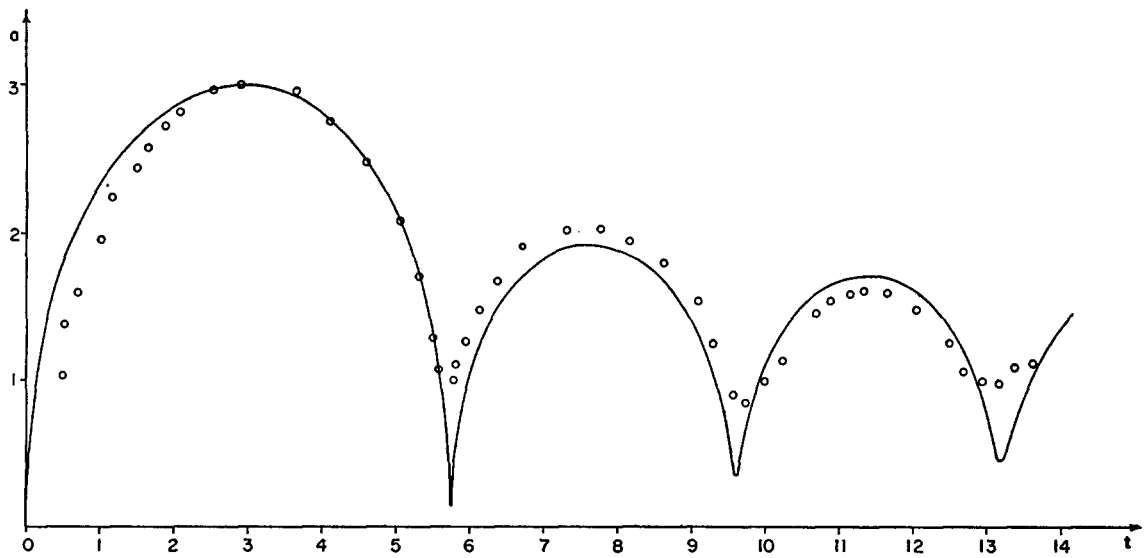

FIG. 7. The bubble radius as a function of time for a 0.55-lb charge of tetryl detonated at a depth of 300 ft below the water surface. The circles are experimental points and the solid curve is calculated from Eq. (28). The unit of length is $\bar{a}=6$ inches and the unit of time is $\bar{a}(\rho p_0^{-1})^{\frac{1}{2}}=4.85$ milliseconds.

for any explosion bubble at one of the four depths in the table. If the initial data (i.e. a_0 and $\dot{a}_0$) for this bubble lie on one of the computed curves for that depth, then the computed curve applies to this bubble from the initial point on. If the initial data is nearly the same as that at a point on one of the computed curves, then the curve applies, approximately, to this bubble.

To see this more clearly, let us consider the (a,v) plane in Fig. 1. Let P be the initial point with the assigned initial values a_0 and $\dot{a}_0$, and let Q be the nearest point to P on a computed spiral. Since the spirals interlace, two spirals which are close to each other at one point will remain close thereafter. Thus if P is close to Q, only a small error will be made in replacing the spiral through P by that through Q. In particular the maxima and minima of the radius and velocity will be accurately predicted. However the error in the (a,t) plane may be somewhat greater since the two curves may get out of phase with each other if many cycles are considered.

In applying the theory to the bubble produced by a given explosive charge, it may suffice to simply choose a_0 as the initial charge radius and $\dot{a}_0=0$. Another convenient possibility is to choose a_0 as the maximum radius given by the incompressible theory and $\dot{a}_0=0$. In units of $\bar{a}$ this maximum is

$$a_0=[(1-\kappa)\epsilon\beta^{-1/\gamma}(p_0^{-1}W)^{\gamma-1/\gamma}]^{\frac{1}{3}}. \tag{31}$$

Here W = charge weight, ϵ = energy per unit charge weight, $\beta=kW^{-\gamma}$ = adiabatic constant and $\kappa=\beta\epsilon^{-\gamma}p_0^{\gamma-1}/(\gamma-1)$. Then the calculation will proceed from the first maximum.

To compare our theory with experiment, we considered a 0.55 lb tetryl charge fired at 300 feet below the water surface, because for this case experimental data are available in [1], p. 271, Fig. 8.1. From this data we estimated that the ultimate bubble radius $\bar{a}=6$ inches. In terms of this unit, the first maximum bubble radius, which was measured as 18 inches, becomes 3. Since the measured data were poor initially, we began our integration from the first maximum using $a_0=3$, $\dot{a}_0=0$, $\gamma=1.25$ and $c=46.5$. We integrated both forward and backward in time from this point. The result is shown in Fig. 7 along with the experimental points. The first oscillation period was calculated to be 27.9 milliseconds, while the measured value was 28 milliseconds. Some of the discrepancy in the radius-time curve is undoubtedly due to error in estimating the ultimate radius $\bar{a}$ from the data.

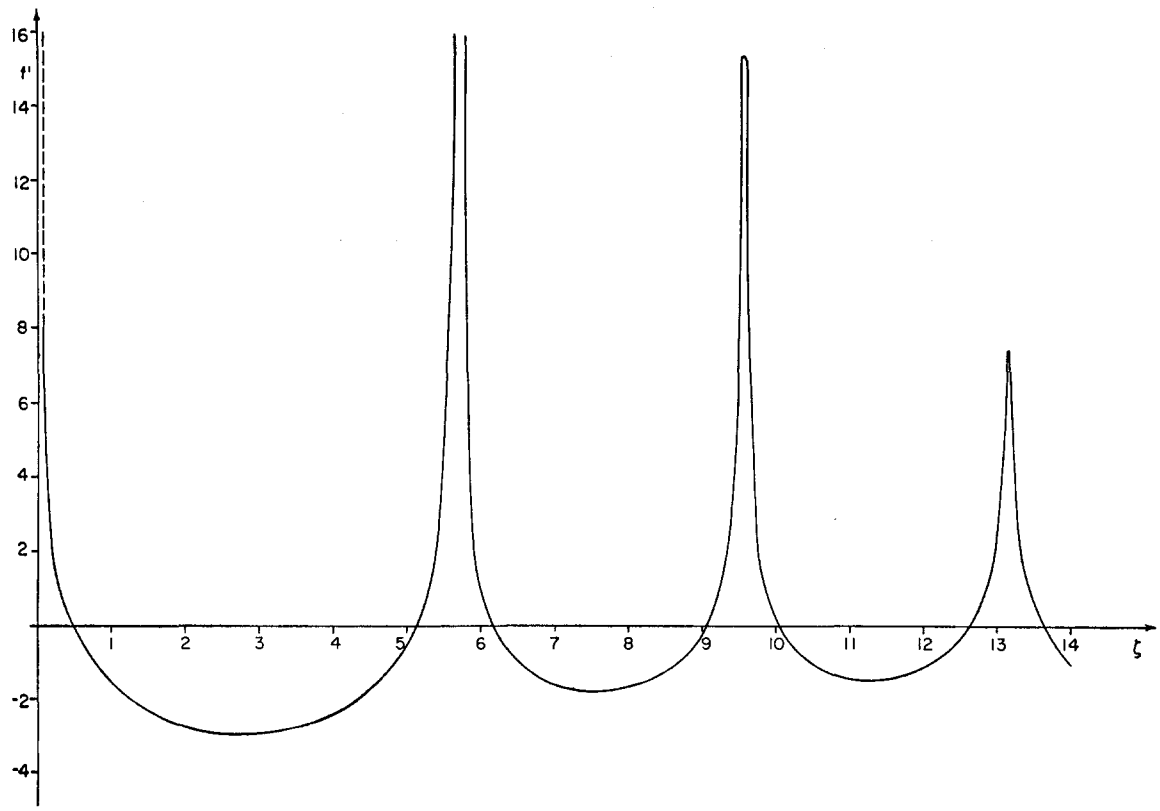

FIG. 8. The pressure in the water as a function of time, due to a 0.55-lb charge of tetryl detonated at a depth of 300 ft. The pressure p at distance r from the explosion is $p\sim p_0-\rho f''/r$ according to Eq. (16). The function $-f'=r\rho^{-1}(p-p_0)$ is plotted here as a function of $\zeta=t-rc^{-1}$. The calculation is based on Eq. (14), and the values of a and $\dot{a}$ obtained in calculating the curve of Fig. 7 were used. The unit of time is 4.85 milliseconds. The peak values of $-f'$ are: $-f'=200$ at $\zeta=0$ (estimated), $-f'=135.0$ at $\zeta=5.72$, $-f'=15.35$ at $\zeta=9.62$, $-f'=7.39$ at $\zeta=13.15$.

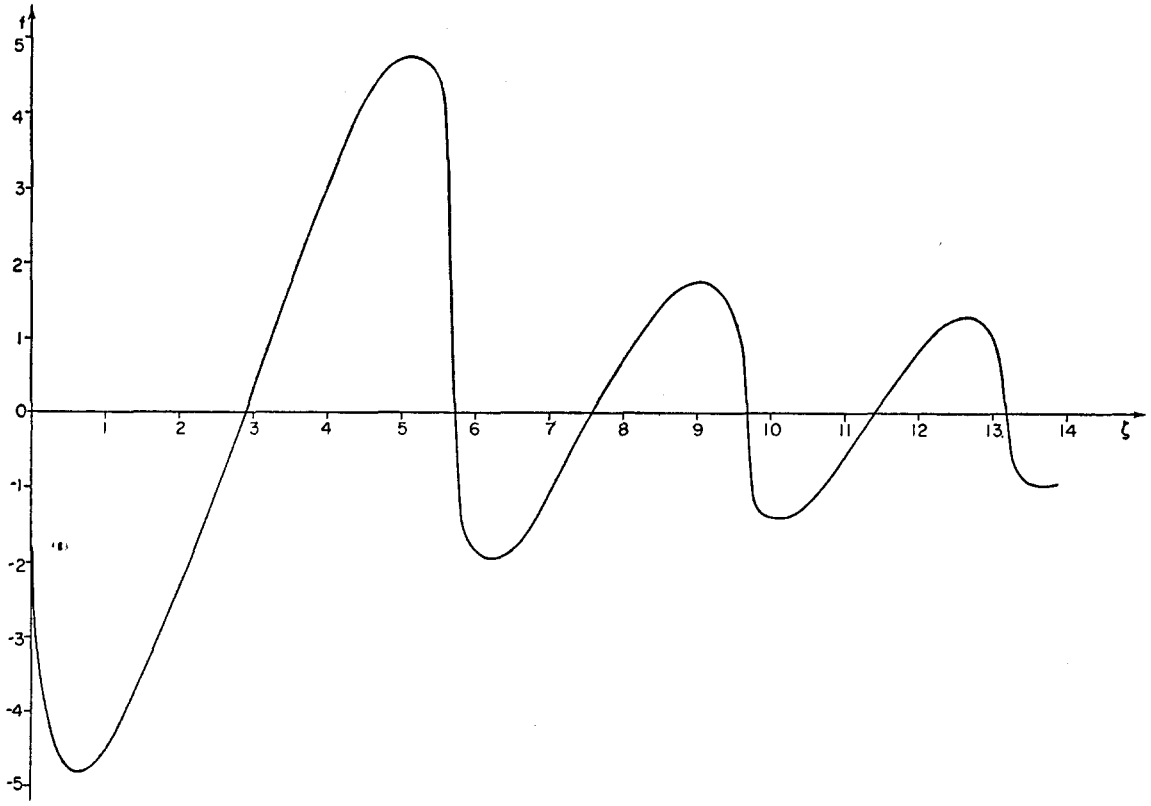

FIG. 9. The function $f(\zeta)$ computed from Eq. (13) using the values of a and $\dot{a}$ obtained in calculating the curve of Fig. 7. Thus it applies to a 0.55-lb charge of tetryl detonated at 300 feet. This function determines the "afterflow" pressure, which is important near the bubble (see Eq. (16)). The unit of time is 4.85 milliseconds.

Using the computed values of $a(t)$, the functions $f(\zeta)$ and $f'(\zeta)$ were computed from (13) and (14). Graphs of these functions are shown in Figs. 8 and 9, respectively. These functions can be used to determine the pressure $p(r,t)$ which is given in (16). In fact, for large distances r, the excess-pressure *vs* time curve is essentially a multiple of the f' curve. For very small distances, however, the other term in (16) may become important, especially between the bubble minima. Yet at $r=6$, i.e. at a distance of two maximum bubble radii, the correction due to the neglected term is at most 0.85 percent which occurs at $\zeta=1.0$.

6. CONCLUSION

We have presented a theory for the oscillation of spherical underwater explosion bubbles which takes account of the compressibility of the water. Our theory predicts damped oscillations of diminishing period, in qualitative agreement with observations. Comparison of the predicted and observed radius-time curves for one particular case shows fairly good agreement between them (Fig. 7). It therefore seems that this theory takes account of the main physical factors effecting these oscillations.

The usual theory of these oscillations does not take account of the compressibility of the water. Consequently it does not permit radiation of energy from the bubble, as our theory does, and therefore it does not predict damping of the oscillations.

Our theory leads to a nonlinear second-order ordinary differential equation for the bubble radius as a function of time. We have integrated this equation numerically in four cases, corresponding to four different explosion depths and initial radii. These curves can also be used for other initial radii.

Once the radius-time curve is known, the pressure wave emitted by the bubble can be computed. It is this pressure which is of major importance in producing explosive damage.